ELSEVIER

Available online at www.sciencedirect.com
SCIENCE DIRECT®

Journal of Crystal Growth 266 (2004) 320–326

JOURNAL OF CRYSTAL GROWTH

www.elsevier.com/locate/jcrysgro

# Effects of induction heating on temperature distribution and growth rate in large-size SiC growth system

Q.-S. Chen*, P. Gao, W.R. Hu

*Institute of Mechanics, Chinese Academy of Sciences, 15 Bei Si Huan Xi Road, Beijing 100080, China*

**Abstract**

For design of large-size silicon carbide (SiC) growth system, it is essential to choose induction heating parameters such as frequency and power. Modeling and simulations have been performed on a 2-in SiC growth system to investigate the effects of induction heating on the temperature distribution and growth rate. For frequencies in the range of 4–20 kHz, it is found that the maximum temperature and growth temperature in the growth system increase with the frequency while keeping the same current in the induction coil. For lower frequency induction heating, it is difficult to achieve high temperatures, which may be essential for the growth of high-quality crystals. It is observed from experiments that the quality of SiC crystals is related to the growth temperature. The SiC growth rates as a function of system pressure for different frequencies have been obtained by the theoretical method.
© 2004 Elsevier B.V. All rights reserved.

*PACS:* 81.05.Hd; 81.10.Aj; 81.10.Bk

*Keywords:* A1. Computer simulation; A1. Growth models; A2. Growth from vapor; A2. Single crystal growth; A3. Physical vapor deposition processes; B2. Semiconducting silicon compounds

## 1. Introduction

Silicon carbide (SiC) crystals of 50–100 mm diameter grown using the method of physical vapor transport (PVT) are now commercially available [1, 2]. The PVT growth of SiC crystals involves sublimation and condensation, chemical reactions, stoichiometry, mass transport, induced thermal stress, as well as defect and micropipes generation and propagation. Since the defects and micropipes in as-grown crystals are directly related to transport phenomena in the crystal growth system, modeling and simulations have been used by different groups of researchers to develop a basic understanding of physical phenomena and to improve the SiC growth process [3–10]. Various degrees of system complexity have been considered by these authors, such as electromagnetic field produced by RF heating, generated heat power in the graphite susceptor, radiation heat transfer, temperature distribution and growth kinetics. Hofmann et al. [3] modeled the temperature distributions for a growth temperature of 2573 K and system pressure of up to 3500 Pa. Pons et al. [4] calculated the electromagnetic field and temperature distribution, and found that the predicted temperatures for the seed and powder surface (2920 and 3020 K) are much larger than the

*Corresponding author. Tel.: 86-10-62564199; fax: 86-10-62615524.

*E-mail address:* qschen@imech.ac.cn (Q.-S. Chen).

0022-0248/$ - see front matter © 2004 Elsevier B.V. All rights reserved.
doi:10.1016/j.jcrysgro.2004.02.061

external temperatures measured at the top and bottom of the crucible (2390 and 2500 K), while the maximum temperature of the insulation foam on its periphery is about 1000 K. The total pressure is around 30 Torr (4000 Pa) and the growth rate is 1.55 mm/h. Egorov et al. [5] modeled the global heat transfer inside the system for SiC growth in a tantalum container. Müller et al. [6] calculated the temperature distributions in inductively heated SiC growth reactors in temperatures of 2373–2673 K, and found that the temperatures in the powder are highly non-uniform, predicted radial variations of 30–50 K along the powder surface. Karpov et al. [7] predicted growth rate in the growth of SiC in tantalum container. Chen et al. [8] proposed a kinetics model for SiC vapor growth, predicted growth rate as a function of temperature, temperature gradient and inert gas pressure, and obtained growth rate profile across the seed surface in a 2-in growth system. The powder charge is modeled as a solid matrix with a porosity and an effective conductivity that accounts for both the conduction and radiation in the powder. Selder et al. [9] introduced a modeling approach for the simulation of heat and mass transfer during SiC bulk crystal growth and compared calculated results with the experimental data. Råback et al. [10] presented a model for the growth rate of SiC sublimation process and estimated the parametric dependencies of the growth rate. Ma et al. [11] modeled the thermal stresses in the growing crystal in a growth system. The growth pressure is 1333 Pa and the temperature at the bottom of crucible is 2200°C.

The mass transport from the charge to seed and the growth kinetics determine the growth rate and the crystal shape. The growth rate is a strong function of the growth temperature, temperature gradient, inert gas pressure, charge properties (particle size, porosity, height), the gap between the charge and seed, and many other parameters. It would be very difficult to design the growth system and develop processes for the growth of 50–100 mm crystals without the help of modeling and simulation. The temperatures in the growth system are strong functions of the current in the induction coil and the frequency. Modeling of the growth process in a 2-in growth system is performed, and the effects of induction heating on the temperature distribution and growth rate are discussed here.

## 2. Mathematical model

A numerical algorithm has been developed that consists of the calculations of radio-frequency, time-harmonic magnetic field generated by the induction heating, radiation heat transfer in the system, as well as the growth kinetics. The electromagnetic field is obtained by solving the magnetic vector potential equations, and the generated heat power density in the graphite susceptor is obtained by using the eddy current theory. The radiative heat transfer is calculated from the integrated equations for radiation. Chemical reactions and transport of gaseous species, Si, $SiC_2$, $Si_2C$ and SiC, are considered. A growth kinetics model that is based on the Hertz–Knudsen equation is used to relate the growth rate to the supersaturation of the rate-determining vapor species.

For low frequency ($f < 1$ MHz), the Maxwell's equations can be simplified using a quasi-steady approximation. It is assumed that the current in the coil is time-harmonic, and heat generation in the graphite susceptor is caused by the eddy currents. The magnetic vector potential theory is used and the magnetic vector potential equation derived from the Maxwell's equations is

$$\nabla \times \left(\frac{1}{\mu_m}\nabla \times A\right) + \varepsilon_m \frac{\partial^2 A}{\partial t^2} + \sigma_c \frac{\partial A}{\partial t} = \mathbf{J}_{coil}, \qquad (1)$$

where $\mathbf{A}$ is the magnetic vector potential, $\mu_m$ is the magnetic permeability, $\varepsilon_m$ is the permittivity, $\sigma_c$ is the electrical conductivity, and $J_{coil}$ is the current density in the coil.

Assuming that the coil and the electromagnetic field are axisymmetric, such that both the current density, $\mathbf{J}_{coil}$, and the magnetic vector potential, $\mathbf{A}$, have only one angular component with an

exponential form

$$\mathbf{J}_{\text{coil}} = \begin{Bmatrix} 0 \\ J_0 e^{i\omega t} + cc \\ 0 \end{Bmatrix} \quad \text{and} \quad \mathbf{A} = \begin{Bmatrix} 0 \\ A_0 e^{i\omega t} + cc \\ 0 \end{Bmatrix}, \tag{2}$$

where i is the complex unit, $\omega$ is the angular frequency, and cc denotes the complex conjugate. The final equation for magnetic potential, $A_0$, is

$$\left(\frac{\partial^2}{\partial r^2} + \frac{1}{r}\frac{\partial}{\partial r} - \frac{1}{r^2} + \frac{\partial^2}{\partial z^2}\right)\left(\frac{A_0}{\mu_m}\right) + \varepsilon_m \omega^2 A_0 - i\omega\sigma_c A_0 = -J_0. \tag{3}$$

In the above equation, the second term in the left-hand side is negligible. The boundary conditions in an axisymmetric system are:

$$A_0 = 0 \quad \text{at} \quad r = 0 \quad \text{and} \quad (r^2 + z^2) \to \infty. \tag{4}$$

The generated heat power density in the graphite susceptor can be obtained using the eddy current theory:

$$q'''_{\text{eddy}} = \tfrac{1}{2}\sigma_c \omega^2 A_0 A_0^*, \tag{5}$$

where * denotes the complex conjugate.

The temperature distribution in the growth system can be calculated using an energy transport equation by considering chemical reactions, latent heat release and radiation:

$$(\rho c_p)_{\text{eff}} \frac{\partial T}{\partial t} = \nabla \cdot (k_{\text{eff}} \nabla T) + q'''_{\text{eddy}} - (q''_{\text{radi}} + q''_{\text{env}})\delta A/\delta V + q'''_{\text{latent}}, \tag{6}$$

where $\rho$ is the density, $c_p$ is the isobaric specific heat, $q''_{\text{radi}}$ is the radiative heat flux normal to the inner surface of a radiation enclosure, and $\delta A$ and $\delta V$are the area over a finite-volume face and the finite volume near the gas/solid interface, respectively. $q''_{\text{env}}$ is the radiative heat flux to the environment. Subscript eff denotes effective. If the growth rate is low, the latent heat release, $q'''_{\text{latent}}$, can be neglected. Radiations inside the crucible and in the top and bottom holes are considered by using the grid-to-grid radiation model [12, 13].

If the three-dimensional effects are negligible, the symmetric condition can be used:

$$\frac{\partial T}{\partial r} = 0 \quad \text{at} \quad r = 0. \tag{7}$$

The environmental condition is

$$T_{\text{env}} = 293\,\text{K}. \tag{8}$$

In the charge, SiC powder dissolves into different species, and the basic components of the evaporation of SiC are Si, $SiC_2$, $Si_2C$ and SiC. The content of the other components of evaporation ($Si_2$, C, $C_2$, $C_3$) in the vapor is insignificant. We assume that the local thermodynamic equilibrium is reached, then the partial pressures of different species in the charge can be obtained [14]. The vapor species is transported from the charge to the seed by the diffusion and the Stefan flow, which is caused by the evaporative phase change of the SiC powder. The vapor species becomes supersaturated near the seed, since the temperatures at the seed is lower than that in the charge.

We assume that the growth rate on the seed surface is proportional to the supersaturation of the rate-determining species. The supersaturation becomes the driving force for the deposition of SiC on the seed. The rate determining species are Si, $SiC_2$ or $Si_2C$ and the rate determining reactions are:

$$SiC_{2(g)} + Si_{(g)} \Leftrightarrow 2SiC_{(s)}, \tag{9}$$

$$Si_2C_{(g)} \Leftrightarrow SiC_{(s)} + Si_{(g)}, \tag{10}$$

where subscripts s and g denote solid and gas, respectively.

For steady growth, we assume that reactions (9) and (10) are taking place at a ratio of 1:$x$. For example, when 1 $SiC_2$ reacts with 1 Si to form 2 SiC, $x$ $Si_2C$ dissolves into $x$ SiC and $x$ Si. Thus the total quantity of Si, $SiC_2$ and $Si_2C$ transported from the charge to seed should be 2, while the growth of SiC should be $2+x$. The growth rate of SiC crystal derived from the Hertz–Knudsen(HK) equation is

$$G_{\text{SiC}} = \frac{(2+x)M_{\text{SiC}}}{\rho_{\text{SiC}}} \alpha \chi_A [p_A(\text{seed}) - p_A^*(\text{seed})], \tag{11}$$

where $p_A^*$ is the equilibrium vapor pressure of gaseous A, $\chi_A = 1/\sqrt{2\pi M_A R T}$, $\alpha$ is the sticking

coefficient which is set as 1 for the present studies, and $M_A$ is the molecular weight of species A. $x$ is related to the ratio of rates of reactions (9) and (10), and is assumed to be 0 here. If $x$ is not zero, one can simply multiply the following calculated growth rates with $(1+x/2)$. The rate-determining species, A, is therefore chosen as $SiC_2$ at $T < 2900\,K$, as Si at $T > 2900\,K$ [14]. Introducing an advective velocity of the species A, the transport of vapor species A can be obtained from a one-dimensional mass transfer equation. In the one-dimensional system, the flux of species A includes the advection term by Stefan flow and the diffusion term. By assuming the flux of the remaining gas species other than species A as zero, the advective velocity of species A can be obtained. For complete formulations, one can refer to Refs. [12, 13]. Furthermore, the vapor pressure at the source is assumed to be the same as the equilibrium vapor pressure. Here the equilibrium vapor pressures of species Si, $SiC_2$, $Si_2C$ and SiC can be taken from Ref. [14].

The transport equations for electromagnetic field and heat transfer are solved using a numerical scheme based on the control volume method [12]. The grid dependence studies of the numerical scheme and comparisons between the numerical predictions and experimental data for different crystal growth processes can be found in Refs. [13, 15].

## 3. Results and discussions

For growing SiC crystals by using the induction heating method, various frequencies are used by different researchers. For an RF power supply system, the power to be delivered is related to the coupling between the coil and susceptor and the frequency, e.g., the power can be increased if the frequency is increased. Here, we consider a growth system with a coil of 5 turns and a frequency of 8 kHz. Assuming the current density $J_0$ is real, the contours of the real part of the magnetic potential $A_0$ for current of 1200 A is shown in Fig. 1(a). The computational domain is set as $-20<z/R_s<20$ and $r/R_s<20$, where the outer radius of the susceptor, $R_s = 0.045\,m$. The magnetic potential almost diminishes at a distance of $20R_s$ from the induction coil. The real part of the magnetic potential reaches maximum around the coil. The contour lines concentrate along the outer surface of the graphite susceptor. As shown in Fig. 1(a), the contour line, $(A_0)_{real} = 4\times10^{-5}\,Wb/m$, bends in the top region of the susceptor, passes through the outer portion of the cylindrical susceptor, and bends again in the bottom region of the susceptor. The graphite susceptor functions as a shield weakening the electromagnetic field inside the susceptor. The imaginary part of the magnetic potential is shown

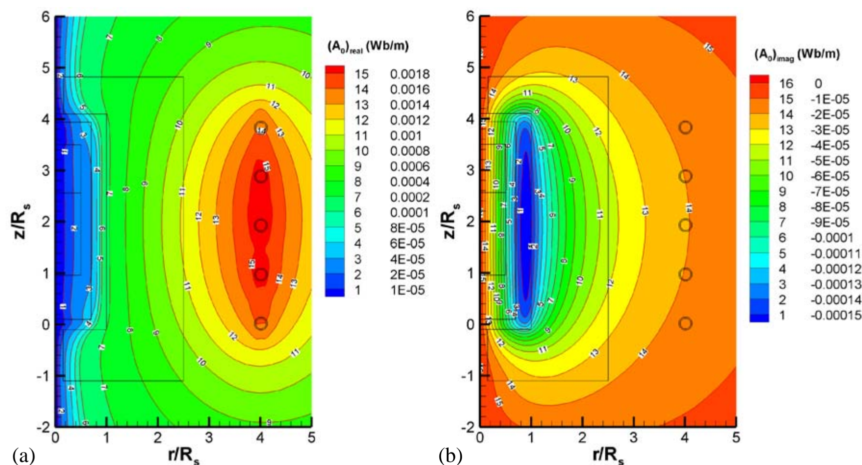


Fig. 1. (a). Contours of the real part of magnetic potential, $(A_0)_{real}$, and (b). contours of the imaginary part of magnetic potential, $(A_0)_{imag}$, for current of 1200 A in the coil and frequency of 8 kHz.

in Fig. 1(b). The absolute value of the imaginary part of the magnetic potential has maximum in the cylindrical graphite susceptor. From Eq. (5), we can see that the main contribution to the power generation in the graphite susceptor is from the imaginary part of the magnetic potential for the present cases.

To investigate the effects of frequency on the temperature distribution, we can keep the current in the coil or the heating power constant. Since there are some power consumptions in the capacitors and the coil, which are cooled by the running water, it is difficult to know what percentage of power goes into the graphite susceptor. However, the current in the coil is related to the voltage, which varies from zero to a certain value, it is possible to calculate the current in the coil from the voltage reading. The temperature distributions in the 2-in system are shown in Fig. 2 for current of 1200 A in the coil and different frequencies. Temperature reaches maximum in the susceptor at the level of the geometric center of the induction coil. The maximum temperature increases with the frequency for the current of 1200 A. Inside the crucible, the temperature has a lower value at the center of the seed because of the cooling effect produced by the top hole. The temperature increases along the radial direction on the seed surface, reaches a high value before the inner wall of the growth chamber. A large radial temperature gradient on the seed surface is important for the enlargement of the seed crystal in the beginning of the growth process. It should be noted that even the radial temperature variation at the seed, about 20 K, is large at the start of the growth, it is still less than the axial temperature variation of about 80 K between the charge and the seed (Fig. 2a). Therefore the assumption that the mass transfer in the growth chamber is predominantly one-dimensional, can be considered valid. The axial temperature gradient in the growth chamber is about 15 K/cm for the 2-in system (Fig. 2a). It should be noted that the temperature gradient in the SiC growth system is related to the thermal design such as arrangement of insulations, and the frequency in the range

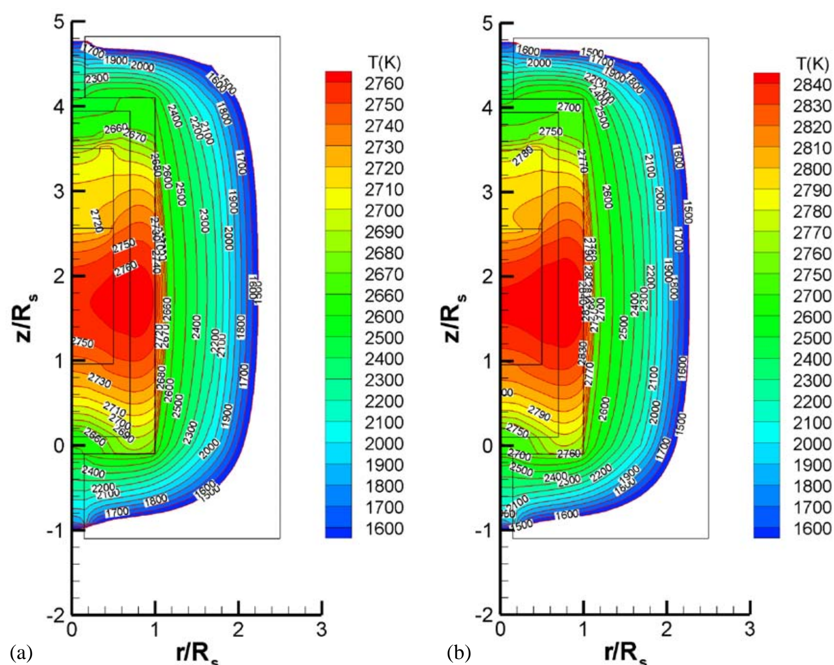


Fig. 2. Temperature distributions in a SiC growth system for current of 1200 A in the coil and (a) frequency of 8 kHz and (b) frequency of 10 kHz.

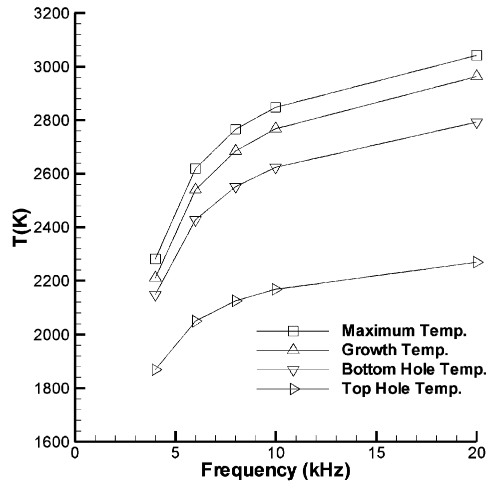


Fig. 3. Dependence of the maximum temperature in the charge, growth temperature at the seed and temperatures measured at the top and bottom holes on the frequency of induction heating.

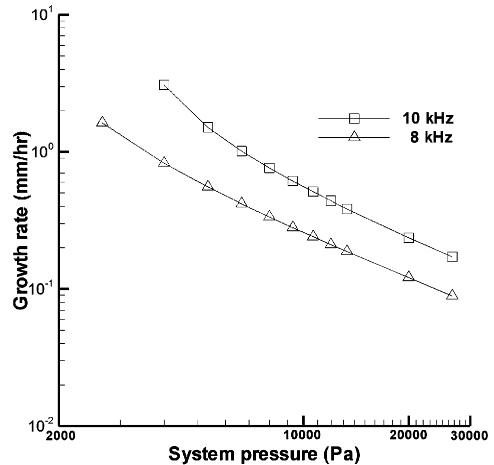


Fig. 4. Dependence of the growth rate on system pressure for current of 1200 A in the coil and frequencies of 10 and 8 kHz.

of 4–20 kHz has less effects on the temperature gradient for the present study.

Fig. 3 shows the dependence of temperatures in the system on the induction frequency. It can be seen that the maximum temperature increases with the frequency. There is a sharp increase of maximum temperature when frequency is increased from 4 to 6 kHz, and a small increase of maximum temperature when frequency is increased from 10 to 20 kHz. It seems the desirable frequency is in the range of 8–10 kHz for the present system. It should be noted that the current in the coil, which is related to the voltage, is limited. The growth rate is related to both the maximum temperature and the growth temperature, or the difference between the maximum temperature and the temperature at the seed. Temperatures at the top and bottom holes can be measured using the infrared pyrometers and be used to control the maximum temperature or the growth temperature in the system during the growth process. For the case of 8 kHz, the maximum temperature is 2766 K while the measured temperature at the bottom hole is 2552 K (Fig. 3). Also for the case of 10 kHz, the maximum temperature is 2848 K while the measured temperature at the bottom hole is 2624 K (Fig. 3). Fig. 4 shows the dependence of the growth rate on the system pressure for frequencies of 8 and 10 kHz. It can be seen from Fig. 4 that the growth rate in the case of 10 kHz is always larger than that in the case of 8 kHz for the same current and pressure when the inert gas pressure is in the range of 4000–30,000 Pa. The growth rate is almost proportional to the reciprocal of the power of pressure when the system pressure is in the range of 4000–30,000 Pa for the present cases. Further experimental studies on the pressure dependence of the growth rate need to be conducted for the present growth system.

## 4. Conclusions

Modeling and simulations have been performed on a 2-in SiC crystal growth system. The effects of induction heating on the temperature distribution and growth rate are discussed. For design of the large-size SiC growth system, it is essential to choose induction heating parameters such as the electrical current in the coil and frequency. For frequencies in the range of 4–20 kHz, it is found that the maximum temperature and growth temperature increase with the frequency while keeping the same current in the coil. For the case of lower frequency induction heating, it is difficult to achieve high temperature, which may be essential for the growth of high quality crystals.

The SiC growth rates for different frequencies and pressures have been obtained by the theoretical method. The growth rate in the case of 10 kHz is always larger than that in the case of 8 kHz for the same current in the coil and the same system pressure for the present system. By using the modeling tool, it is easy to optimize the parameters that are essential for the growth of high quality and large size SiC crystals. For example, we can predict the temperature distribution by just measuring temperatures at the top hole or the bottom hole. We can know how the thermal design be changed to get the required temperature and temperature gradient and how the growth pressure be chosen to have a high growth rate for the present thermal design. The present system can be used to grow 3-in crystals by modifying the thermal design.

## Acknowledgements

The research was supported by the Knowledge Innovation Program of Chinese Academy of Sciences, and the authors would like to thank Prof. V. Prasad at the Florida International University for helpful discussions.

## References

[1] St.G. Müller, R.C. Glass, H.M. Hobgood, V.F. Tsvetkov, M. Brady, D. Henshall, J.R. Jenny, D. Malta, C.H. Carter Jr., J. Crystal Growth 211 (2000) 325.
[2] C.M. Balkas, A.A. Maltsev, M.D. Roth, N.K. Yushin, Mater. Sci. Forum 338–342 (2000) 79.
[3] D. Hofmann, M. Bickermann, R. Eckstein, M. Kölbl, St.G. Müller, E. Schmitt, A. Weber, A. Winnacker, J. Crystal Growth 198/199 (1999) 1005.
[4] M. Pons, M. Anikin, K. Chourou, J.M. Dedulle, R. Madar, E. Blanquet, A. Pisch, C. Bernard, P. Grosse, C. Faure, G. Basset, Y. Grange, Mater. Sci. Eng. B61–62 (1999) 18.
[5] Yu.E. Egorov, A.O. Galyukov, S.G. Gurevich, Yu.N. Makarov, E.N. Mokhov, M.G. Ramm, M.S. Ramm, A.D. Roenkov, A.S. Segal, Yu.A. Vodakov, A.N. Vorob'ev, A.I. Zhmakin, Mater. Sci. Forum 264–268 (1998) 61.
[6] St.G. Müller, R.C. Glass, H.M. Hobgood, V.F. Tsvetkov, M. Brady, D. Henshall, J.R. Jenny, D. Malta, C.H. Carter Jr., J. Crystal Growth 211 (2000) 325.
[7] S.Yu. Karpov, A.V. Kulik, I.A. Zhmakin, Yu.N. Makarov, E.N. Mokhov, M.G. Ramm, M.S. Ramm, A.D. Roenkov, Yu.A. Vodakov, J. Crystal Growth 211 (2000) 347.
[8] Q.-S. Chen, H. Zhang, V. Prasad, J. Crystal Growth 224 (2001) 101.
[9] M. Selder, L. Kadinski, Yu. Makarov, F. Durst, P. Wellmann, T. Straubinger, D. Hofmann, S. Karpov, M. Ramm, J. Crystal Growth 211 (2000) 333.
[10] P. Råback, R. Nieminen, R. Yakimova, M. Tuominen, E. Janzén, Mater. Sci. Forum 264–268 (1998) 65.
[11] R.-H. Ma, H. Zhang, S. Ha, M. Skowronski, J. Crystal Growth 252 (2003) 523.
[12] Q.-S. Chen, H. Zhang, V. Prasad, C.M. Balkas, N.K. Yushin, J. Heat Transfer 123 (2001) 1098.
[13] Q.-S. Chen, H. Zhang, V. Prasad, J. Crystal Growth 230 (2001) 239.
[14] S.K. Lilov, Mater. Sci. Eng. B21 (1993) 65.
[15] A. Roy, B. Mackintosh, J.P. Kalejs, Q.-S. Chen, H. Zhang, V. Prasad, J. Crystal Growth 211 (2000) 365.